

# Modeling of a Solar Air Heater with Sensible Thermal Storage and Natural Draft

Shadreck M. Situmbeko

University of Botswana, Gaborone, Botswana;  
University of KwaZulu-Natal, Durban, RSA;

Freddie L. Inambao

University of KwaZulu-Natal, Durban, RSA;

Kris L. Kumar

University of Botswana,  
Gaborone, Botswana;

**Abstract-**The paper presents a novel system of employing reverse thermosyphon flow in order to create round-the-clock operation of a solar air heating system with a sensible thermal storage. In the proposed system, heating of air is achieved in the day through direct solar thermal heating; thereafter, heating is achieved in the night through reverse thermosyphon flow from the thermal storage; thus keeping the water-ethylene-glycol storage in motion at all times. The innovative technique has been shown to result in operating the solar air heater on a continuous basis over the 24 hours cycle. In doing so, it is also established that 50/50 water and glycol mixture is ideally suited to serve as the solar thermal energy storage and release medium. Basic principles of fluid dynamics and heat transfer are employed to study the flow of heat storage fluid in either direction in keeping with the thermal gradient during day and night. Conceptual framework is reinforced by solving the equations of motion through computer simulation on the one hand and designing and operating a prototype on the other. Both the computer simulation model and physical model establish the authenticity of the proposal. Optimization of some important operating parameters such as plate spacing, concentration of the water ethylene glycol heat transfer fluid and the draft height has also been undertaken.

**Key words:** reverse thermosyphon, solar air heating, sensible thermal storage, water-ethylene-glycol.

## Nomenclature

### Roman Symbols

A	area
a	ambient
c	cover
$c_p$	specific heat at uniform pressure
D	diameter
g	acceleration due to gravity
h	heat transfer coefficient
I	radiation
k	conductivity
L	length
l	longitudinal
$L_{ins}$	insulation thickness
m	mean
$\dot{m}$	mass flow rate

Nud	Nusselt number for flow in a pipe
Nup	Nusselt number for flow in between two flat plates
P	pressure
$\dot{Q}$	rate of heat transfer
Re	Reynold's number
T	temperature

### Greek Symbols

$\alpha$	absorptivity
$\Delta$	delta (mathematical symbol)
$\varepsilon$	emissivity
$\theta$	angle of inclination
$\mu$	dynamic viscosity
$\rho$	density
$\tau$	transmissivity

### Abbreviations

abs	absorber
conv.	convection
I.D	internal diameter
ins	insulation
sol	solar
$\dot{v}$	volumetric flow rate

## I. INTRODUCTION

This research has come about as an offshoot of a larger project on the research and development of a solar chimney, whose ultimate aim was to develop a working solar chimney plant to be constructed and installed for supplying power to a remote village in Botswana by 2016 [1]. The task was conducted as a consultancy cum joint-research by the authors from the University of Botswana (UB) with the then Botswana Technology Centre (BOTECH). The work was based on the research and development of a solar thermal storage model that could be integrated into the existing small 20 m height solar chimney plant at the BOTECH. A comprehensive survey was undertaken to study the literature and state of art of solar chimney research. It was soon realised that the major

problem was the inadequacy of solid storage devices in their inability to create a continuous thermal heating of air during day and night. It led the authors to conceive liquid storage systems, which are also more effective in terms of heat transfer and cost minimisation. The modelling process consisted of development of both mathematical (and computer simulations) and physical models. Finally, the paper presents a validation of the theoretical results by comparing with a sizable sample of experimental observations. A fair degree of agreement between the two is a pointer to the validity of the proposed model.

## II. LITERATURE SURVEY

A comprehensive literature survey and consultations with industry and academia including a visit to University of Stellenbosch were undertaken; an abridged historical perspective is included here whereas other aspects including mathematical theories and empirical formulae are included in respective sections of the paper.

Solar collectors can typically be broadly classified as thermal collectors converting solar radiation into heat energy or photovoltaic converting solar radiation directly into electric energy. Tremendous strides have been made in the development of both types dating back to 1839 when the photovoltaic was first discovered [2] and 1767 when the solar thermal collector was first developed [3]. PVT for solar photovoltaic and thermal hybrid system is a technology convergence application combining the generation of electricity as well as space heating through air heating [4]. In this study we investigate a combined solar thermal air-and-water heating hybrid application; where the air is available immediately for use whilst the water is used as a storage medium available for space heating at later hours when solar radiation is not available.

## III. SOLAR ENERGY SCENARIO IN BOTSWANA

The location of the study was Gaborone with coordinates  $24^{\circ} 39' 29''$  S and  $28^{\circ} 54' 44''$  E; Gaborone is a city in Botswana, Southern Africa. Botswana lies in the most favourable sunbelts; lying between latitudes  $15^{\circ}$ N, and  $35^{\circ}$ N, as also  $15^{\circ}$ S, and  $35^{\circ}$ S. These semi-arid regions are characterized by having the greatest amount of solar radiation, more than 90% of which comes as direct radiation because of the limited cloud coverage and rainfall. Moreover, there is usually over 3,000 hours of sunshine per year.

Gaborone has on average 74 days per year with temperatures above  $32^{\circ}$  C, 196 days per year with temperatures above  $26^{\circ}$  C and 51 days per year with temperatures below  $7^{\circ}$  C. There is on average one day per year with temperatures below  $0^{\circ}$  C. The average dew point peaks around January and February at  $16^{\circ}$  C and hits the lowest levels in July at  $2^{\circ}$  C. The average dew point in a given year is  $10^{\circ}$  C.

Solar radiation level at Gaborone is  $14.6$  MJ/m<sup>2</sup> in June and  $26.2$  MJ/m<sup>2</sup> in December, giving an average of  $21$  MJ/m<sup>2</sup>[5].

## IV. THERMAL STORAGE MEDIUM

The result of the survey of thermal storage methods and media as well as a wide search and consulting strategy that included a visit to Stellenbosch University was that the most

appropriate storage system would have to be based on a sensible thermal storage employing a liquid such as water or more specifically a water-ethylene-glycol mixture as the storage media [6]. The selection was based on the comparison of several sensible thermal storage materials as represented in figure 1; the figure shows a comparison of thermal masses of various sensible storage materials and water appears to be most promising.

Further an analysis was undertaken of the following advantages and disadvantages associated with the use of water as a storage medium:

Advantages:

- (i) Water is most inexpensive, easy to handle, non-toxic, non-combustible and widely available.
  - (ii) Water has the highest specific heat and high density.
  - (iii) Heat exchangers are not necessary if water is used as the heat carrier in the collector.
  - (iv) Natural convection flows can be utilized when pumping energy is scarce.
  - (v) Simultaneous charging and discharging of the storage tank is possible.
  - (vi) Adjustment and control of a water system is easily variable and flexible.
- Disadvantages:
- (viii) Water might partially freeze at very low temperature or partially boil when very hot.
  - (ix) Water is highly corrosive to normally used materials.
  - (x) Working temperatures are limited to less than  $100^{\circ}$ C.
  - (xi) Water is difficult to stratify, if required.

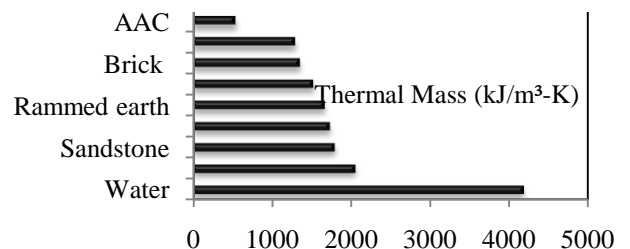


Fig. 1: Comparison of thermal masses of storage materials  
(Note: AAC=Autoclaved Aerated Concrete; FC=Fibre Cement)

The thought of water-glycol mixture emerged from the fact that ethylene glycol is a good antifreeze agent and ethylene-water mixture has been tried successfully in cold climate. It is also noted that addition of ethylene to water does not result in loss of advantages of using water, except for nominal additional cost because, once added, the mixture remains circulating in the system. Water is a good candidate as per its advantages but in case the temperature drops too low, it may partially freeze and if the temperature rises too high, it may even become steam resulting in steam-lock; hence water-glycol is recommended.

It was also established that such a system would have to be passive, not employing any driving devices (such as pumps) requiring external power supply; as such it was envisaged that such a system would have to rely on thermosyphon flow and reverse-thermosyphon depending on the thermal gradient at a given instant.

V. CONCEPTUALISATION OF THE SYSTEM

Observation of existing tubular solar water heaters shows that the heated water rises up the inclined tubes and it is stored in the tank provided atop. It was also noted that it is often necessary to install a one-way valve in order to check the water from returning down. The authors studied the system closely and discovered that, during the process of solar heating, water cannot flow down but after the hot water is stored in the tank atop and solar heating has ceased, it tends to flow back. This phenomenon, called reversed thermosyphon, is the one which is desirable to heat the air during the part of the cycle when solar heating is not available.

In terms of fluid mechanics, reverse circulation in thermosyphon solar water heating systems refers to a type of flow whereby the heated water stored in the tank on account of lower density flows back to the solar collector and thereby loses heat to the ambient. Such thermal losses will normally be dictated by the differences between the temperatures of the collector-water, storage-water as well as the ambient and sky temperatures. It is to avoid the undesired reverse flow that conventional passive solar water heating systems usually have a non-return valve installed in the pipe connecting the top of the collector and the inlet to the tank; some other systems are designed or installed such that there is ample geometrical separation in the vertical heights of the top of the collector and the bottom of the tank; the separation is usually in the range of 200 to 500 mm [7]. In our system, the design is deliberately made to promote reverse thermosyphon in the non-solar hours by not incorporating a non-return valve and positioning the bottom level of the storage tank at or below the top of the collector.

The conceptualised model, therefore, consists of a standard solar collector with the lower and upper ends of the collector box removed; thus the collector doubles as a natural convection air heater as well as a water heater. The heated water is stored in the tank at the top of the collector as in figure 2. The overall dimensions of the collector are shown in figure 3.

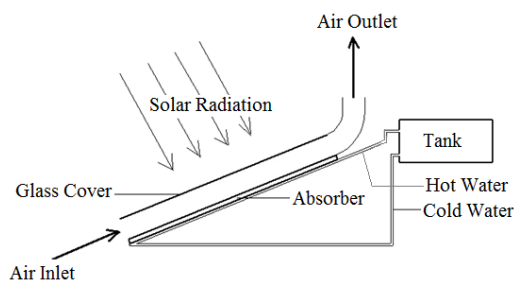


Fig. 2. Solar air heater with water as thermal storage medium

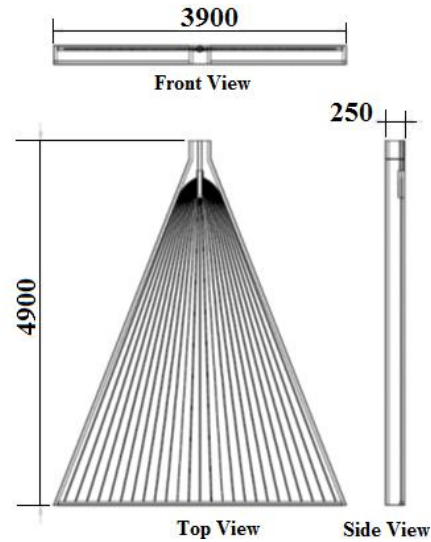


Fig. 3. Overall dimensions of the solar air heater (in mm)

The specification of the materials and their optical and thermal characteristics are shown in tables 1 and 2 as follows:

TABLE 1: MATERIAL CHARACTERISTICS OF THE COLLECTOR MODEL

absorber plate	1mm aluminium plate
riser pipes	I.D 6mm by 1mm copper pipe; number of riser pipes = 25.
insulation	40mm polyurethane foam
transparent cover	4mm solar grade glass
heat transfer fluid	water-ethylene glycol
size of storage tank	300 litres

TABLE 2: OPTICAL AND THERMAL CHARACTERISTICS OF THE COLLECTOR MODEL

absorber absorptivity	$\alpha_{abs} = 0.9$
absorber emissivity	$\epsilon_{abs} = 0.1$
cover emissivity	$\epsilon_c = 0.85$
cover transmissivity	$\tau_c = 0.9$
insulation conductivity	$k_{ins} = 0.023 \text{ W/m-K}$
wind convection coefficient	$h_{c-a} = 5.0 \text{ W/m}^2\text{-K}$
heat transfer fluid Nusselt number, heat transfer fluid flow determined to be laminar	$Nud_{wg} = (3.66 + 4.36)/2$
air flow Nusselt number	$Nup_{air}$ - interpolated from a table [8] for laminar flow; for turbulent flow it is given by equation: $Nup = 0.0158 * Re_{air}^{0.8}$ where $Re_{air}$ is Reynold's number

It is noted here that depending on the level of accuracy required the optical properties maybe modelled to vary with the solar radiation incident angle, such that that  $\tau(\theta)$ ,  $\alpha(\theta)$ ; [9].

#### IV. MATHEMATICAL MODEL OF THE SYSTEM

The mathematical model of the system is developed based on the segmented model of the air heater with water-glycol mixture as the storage material:

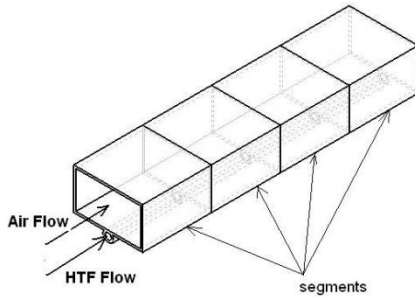


Fig.4. Segmented model  
(HTF (heat transfer fluid) refers to water-glycol mixture)

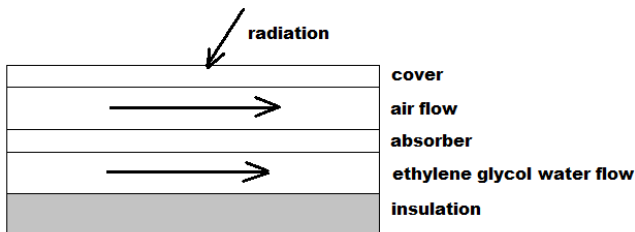


Figure 5: One segment model

Figure 6 shows the energy balance for the absorber segment. The energy balance is represented mathematically by equations 1 and 2.

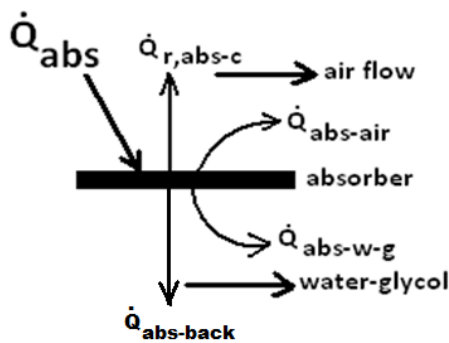


Fig.6. Absorber segment heat transfer model

$$\dot{Q}_{abs} = \dot{Q}_{abs-air} + \dot{Q}_{abs-wg} + \dot{Q}_{r,abs-c} + \dot{Q}_{abs-back} \quad (1)$$

$$\dot{Q}_{abs} = \tau_c * \alpha_{abs} * A_{abs} * I_{sol} \quad (2)$$

The energy balance for the cover segment is shown in figure 7 and is given by equations 3 to 8.

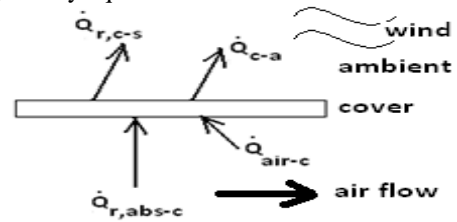


Fig. 7. Cover segment heat transfer model

$$\dot{Q}_{air-c} + \dot{Q}_{r,abs-c} = \dot{Q}_{c-a} + \dot{Q}_{r,c-sky} \quad (3)$$

$$\dot{Q}_{r,abs-c} = h_{r,abs-c} * A_c * (T_{abs} - T_c) \quad (4)$$

$$\dot{Q}_{air-c} = h_{air-c} * A_c * (T_{m,air} - T_c) \quad (5)$$

$$\dot{Q}_{r,c-sky} = \epsilon_c * \sigma * A_c * (T_c^4 - T_{sky}^4) \quad (6)$$

$$\dot{Q}_{c-a} = h_{c-a} * A_c * (T_c - T_a) \quad (7)$$

$$T_{sky} = 0.0552 * T_a^{1.5} \quad (8)$$

The energy balance on the air flow segment is represented by figure 8 and equations 9 to 13.

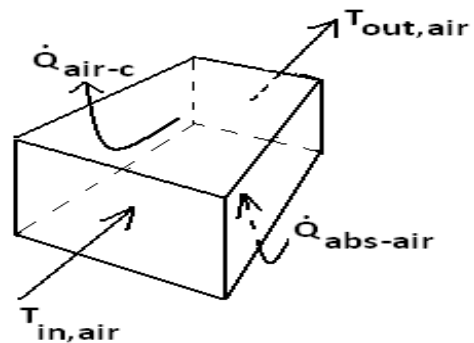


Fig.8. Air flow segment heat transfer model

$$\dot{Q}_{abs-air} - \dot{Q}_{air-c} = \dot{Q}_{air} \quad (9)$$

$$\dot{Q}_{abs-air} = h_{abs-air} * A_{abs} * (T_{abs} - T_{m,air}) \quad (10)$$

$$\dot{Q}_{air-c} = h_{air-c} * A_c * (T_{m,air} - T_c) \quad (11)$$

$$\dot{Q}_{air} = \dot{m}_{air} * c_{p,air} * (T_{out,air} - T_{in,air}) \quad (12)$$

$$h_{air-c} = h_{abs-air} \quad (13)$$

Figure 9 and equations 14 and 15 show the energy balance on the water-ethylene-glycol flow segment.

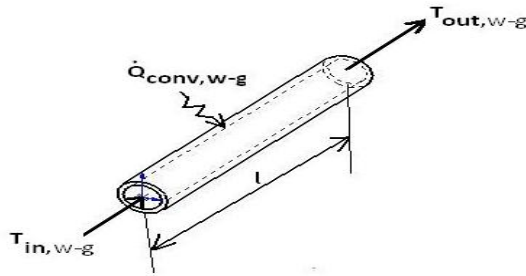


Fig.9. Water ethylene-glycol flow segment heat transfer model

$$\dot{Q}_{conv,wg} = \dot{m}_{wg} * c_{p,wg} * (T_{out,wg} - T_{in,wg}) \quad (14)$$

$$\dot{Q}_{conv,wg} = h_{abs-wg} * A_{l,wg} * (T_{abs} - T_{m,wg}) \quad (15)$$

The thermosyphon model is based on Poiseuille’s Law for laminar flow and is shown in equations 16 and 17:

$$v \dot{\omega} l = \pi \left(\frac{D}{2}\right)^4 * \frac{\Delta P}{8 \mu L} \quad (16)$$

$$\Delta P = g * \Delta \rho * L * \sin \theta \quad (17)$$

The total energy incident on the absorber, total energy transferred to the air, and total energy transferred to the heat transfer fluid are obtained by summations of the segment energies as in the following set of equations; number 18 below:

$$\begin{aligned} \dot{Q}_{abs} &= \sum_{i=1}^{i=N} \dot{Q}_{abs}(i) \\ \dot{Q}_{air} &= \sum_{i=1}^{i=N} \dot{Q}_{air}(i) \\ \dot{Q}_{w-g} &= \sum_{i=1}^{i=N} \dot{Q}_{w-g}(i) \end{aligned} \quad (18)$$

The draft required to promote air flow is represented by the Boussinesq approximation. In particular the air flow exit velocity is modeled by equation 19 as:

$$V_{Nn} = \sqrt{2gH \left(\frac{T_{air,Nn} - T_a}{T_a}\right)} \quad (19)$$

Where H is included as if there were a chimney,  $T_{air,Nn}$  is the temperature of the air flow exiting the collector and  $T_a$  is the ambient temperature (also equals the temperature of the air flow entering the collector)

The thermal storage model consists of an energy balance consisting of Charging, Discharging and Thermal Losses. In this model thermal losses are assumed insignificant. That means during ‘Day Time Simulation’ the storage model assumes the ‘Charging Mode’ and during the ‘Night Time Simulation’, the ‘Discharging Mode’. Reverse thermosyphon

is assumed for the ‘Discharging Mode’. A further assumption made is that there is no stratification in the storage tank, that is, the storage has one uniform temperature.

The charging model is given by equations 20 and 21:

$$\dot{Q}_{tank} = \dot{m}_{wg} * C_{p_{wg}} * (T_{wg,out,Nn} - T_{tank}) \quad (20)$$

$$\dot{Q}_{tank} = m_{wg,tank} * C_{p_{wg}} * \left[\frac{T_{tank} - T_{wg,in,0}}{t_{cycle}}\right] \quad (21)$$

Where  $\dot{Q}_{tank}$  is the heat transfer rate to the thermal storage;  $\dot{m}_{wg}$  is the mass flow rate of the water ethylene glycol working fluid;  $m_{wg,tank}$  is the mass of the water ethylene glycol in the storage tank;  $C_{p_{wg}}$  is the specific heat capacity of the water ethylene glycol and  $t_{cycle}$  is the cycle time. The other parameters  $T_{wg,out,Nn}$ ,  $T_{wg,in,0}$  and  $T_{tank}$  are temperatures of the working fluid exiting the collector model and entering the storage tank, of the working fluid entering the collector model at the previous cycle (also the previous storage tank temperature) and the new storage tank temperature respectively.

The discharging model is given by the equations 22 and 23:

$$\dot{Q}_{tank} = \dot{m}_{wg} * C_{p_{wg}} * (T_{wg,out,0} - T_{tank}) \quad (22)$$

$$\dot{Q}_{tank} = m_{wg,tank} * C_{p_{wg}} * \left[\frac{T_{tank} - T_{wg,in,Nn}}{t_{cycle}}\right] \quad (23)$$

Where the reversed flow now means that  $T_{wg,out,0}$  and  $T_{wg,in,Nn}$ , and are now temperatures of the working fluid exiting the collector model and entering the storage tank, and of the working fluid entering the collector model at the previous cycle (also the previous storage tank temperature) respectively.

The decision to use averaged figures was based on available climatic data which is based on hourly records as such it an hourly model-based solar radiation model was adopted for the computer simulations as follows:

The total hourly radiation can be estimated from the average daily radiation by using the following equation:

$$I_{sol} = H * r_t \quad (24)$$

The coefficient to convert total daily radiation to total hourly radiation is given by equation 25:

$$r_t = \frac{\pi}{24} (a + b \cos w) \frac{\cos w - \cos w_s}{\sin w_s - \frac{\pi w_s}{180} \cos w_s} \quad (25)$$

Where ‘w’ is the hour angle and ‘w<sub>s</sub>’ is the sunset hour angle in degrees. The coefficients ‘a’ and ‘b’ are given by equations 26:

$$\begin{aligned} a &= 0.409 + 0.5016 \sin(w_s - 60) \\ b &= 0.6609 - 0.4767 \sin(w_s - 60) \end{aligned} \quad (26)$$

Two wind convection coefficients were considered for the study; however due to unavailability of wind speed data the simplification was made to use a constant wind coefficient value:

For the Wind Convection Coefficients, Duffie and Beckman[10] recommend using equation 27; that is, the greater of the two coefficients in the parenthesis:

$$h_w = \max \left[ 5, \frac{8.6V^{0.6}}{L^{0.4}} \right] \quad (27)$$

where V is wind speed and L is the cube root of the house volume.

Another wind coefficient is based on Jurges Equation [11]:

$$h_w = 2.8 + 3.8V; V < 5m/s \quad (28)$$

## VII. COMPUTER MODEL AND SIMULATION STUDIES

The set of equations was compiled into an Engineering Equation Solver (EES) code. Computer simulations have been performed and the results are shown in section. [12]

## VIII. VALIDATION OF THE THEORETICAL RESULTS

A prototype was designed and constructed and tested. The prototype was in the form of 'a segment' of the intended solar water heater as shown in figures 10 to 12 [13]. The prototype was considered adequate because the same segment could be placed in different orientations and the results compounded to represent the total heating system. Sample experiments, with limited orientations in order to represent the overall system adequately were conducted and data recorded. Comparison of the sample experimental results with those predicted theoretically showed fair agreement within the limits of experimental error. The theoretical computations were thus validated to the extent tested.



Fig.10. One panel test setup



Fig.11. Showing the Delta-T datalogger

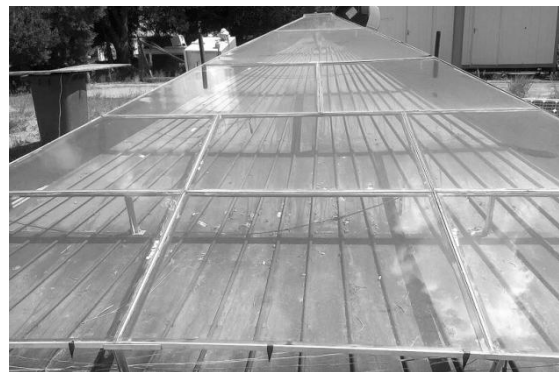


Fig. 12. Showing the riser pipes and instrumentation wiring

## IX. RESULTS

The preliminary results are presented in the following charts of figures 13 to 18.

The first set of results was for testing the thermosyphon and reverse thermosyphon effects; this was done at plate spacing of 200mm and water ethylene glycol concentration of 50%; and simulations were performed for a 24 hours period. The results are shown in figures 13 and 14; figure 13 shows the temperature variation of the air and water at one hour intervals over a 24 hour cycle; figure 14 is a magnified view of figure 13 and only shows the part where the temperature in the storage tank becomes higher than the temperatures of both the absorber plate and of the heat transfer fluid flowing in the absorber runners thus depicting the reversal of energy transfer from solar hours to non-solar hours at 18 hours in the evening. Note that the air inlet temperature was equated to the hourly ambient air temperature data obtained from website <http://www.timeanddate.com/weather/botswana/gaborone/hourly> [14].

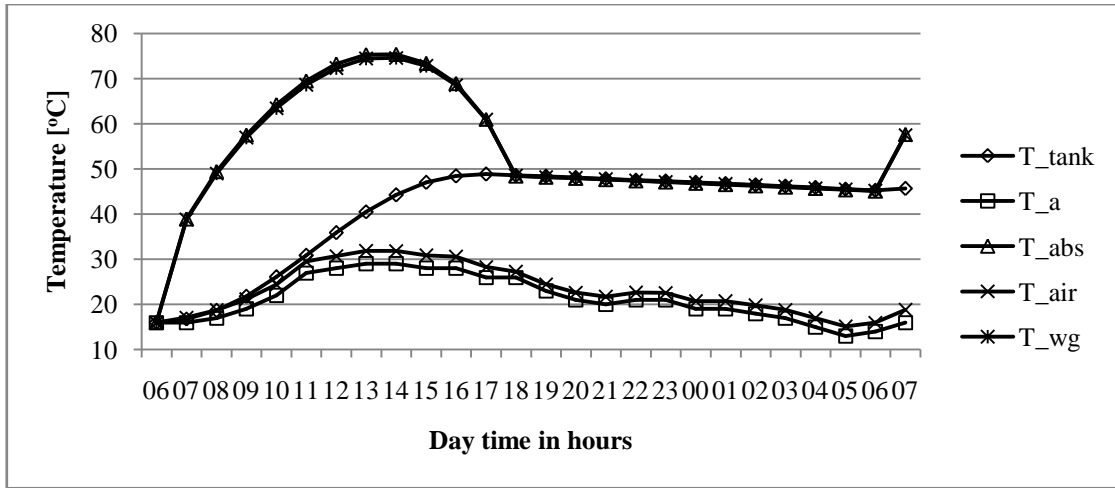


Fig. 13 Temperature Variation of Air and Water at One-Hour Intervals

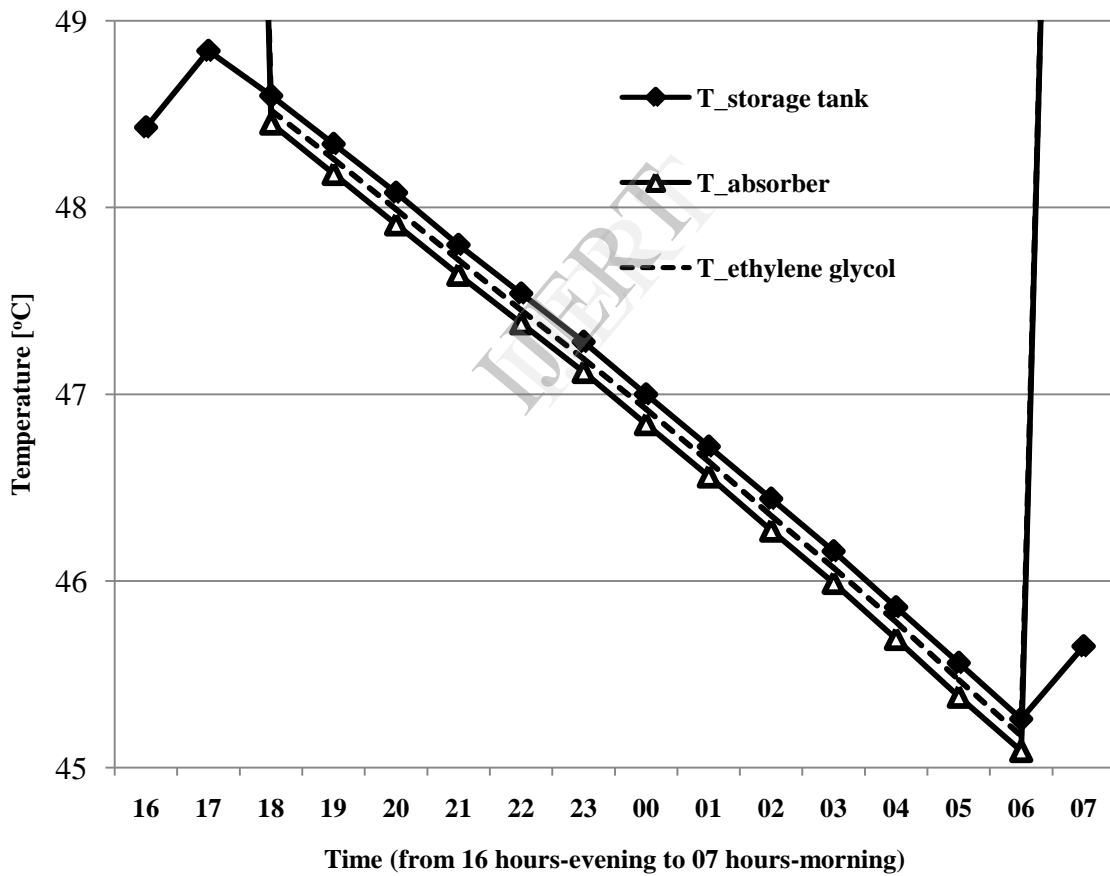


Fig. 14.Reversal of energy transfer from solar hours to non-solar hours

The second set of results is shown in figures15 and 16; this test is part of the optimization process to determine the optimal operating parameters. In this case the parameter being investigated is the plate spacing; the spacing is varied

from 5mm up to 1000mm. The percentage concentration of water ethylene glycol and the draft height are respectively maintained at 50% and 20m.

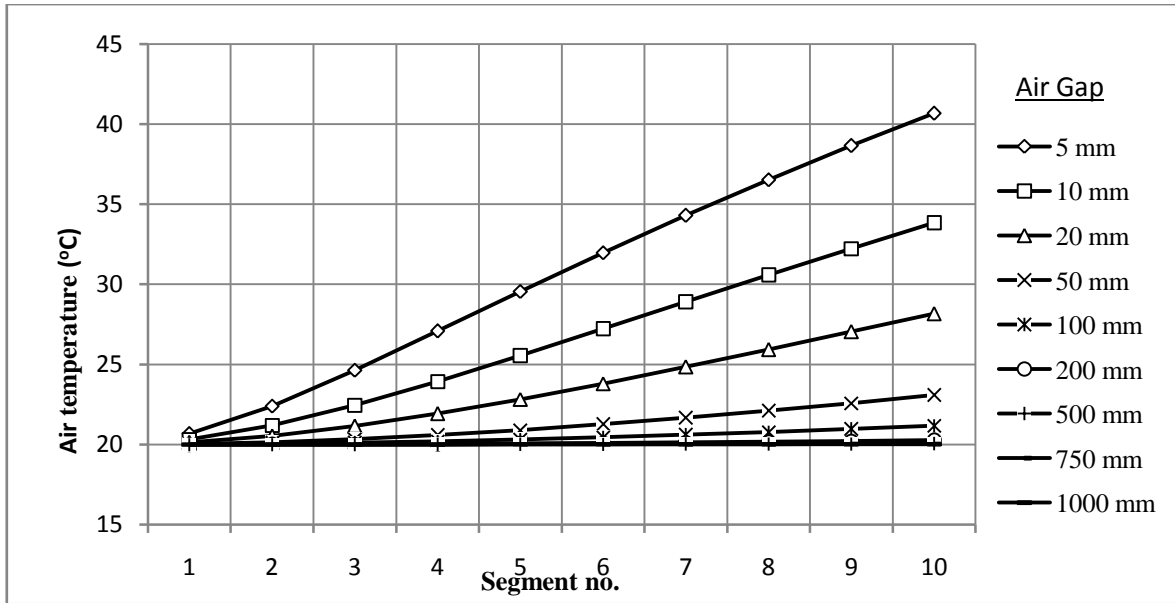


Fig.15.Segment air flow temperature profile for varying air gap

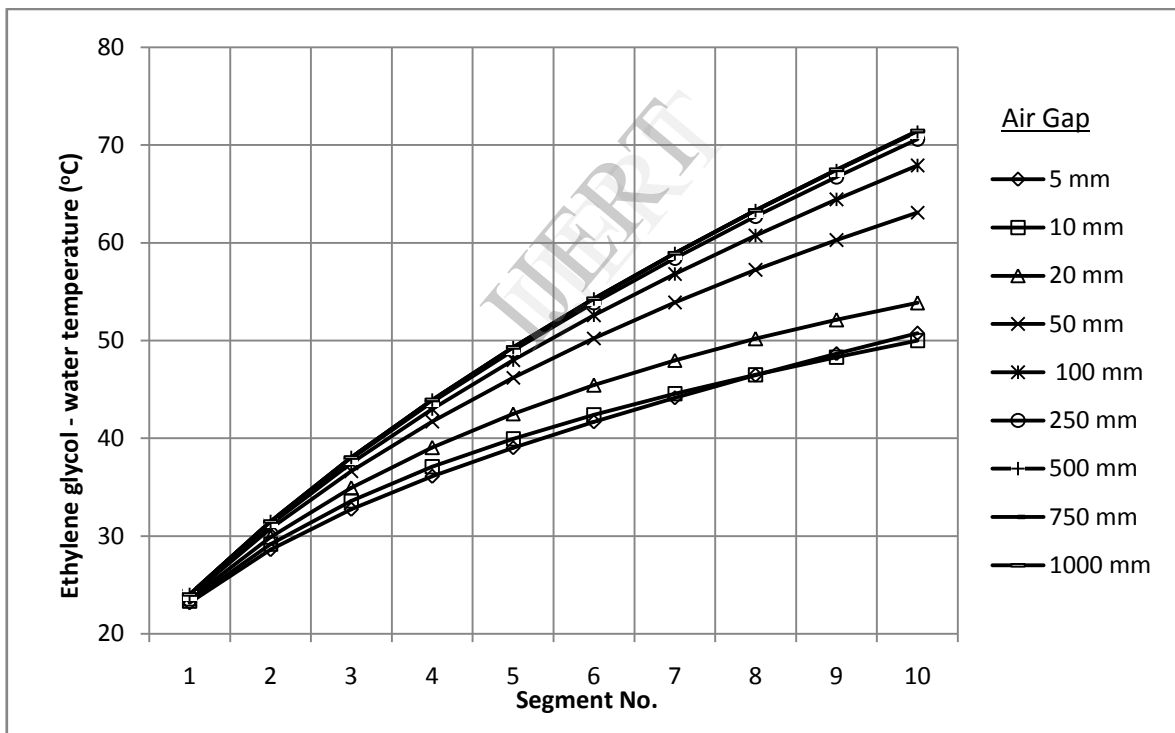


Fig.16.Segment water – ethylene glycol flow temperature profile for varying air gap

The third set of results are for optimising the concentration; the lower and upper limits of the concentration are set at 25% and 60% respectively as is

normally the practice ; the plate spacing for the results shown in figure 17 is maintained constant at 5mm and the draft height at 20m.

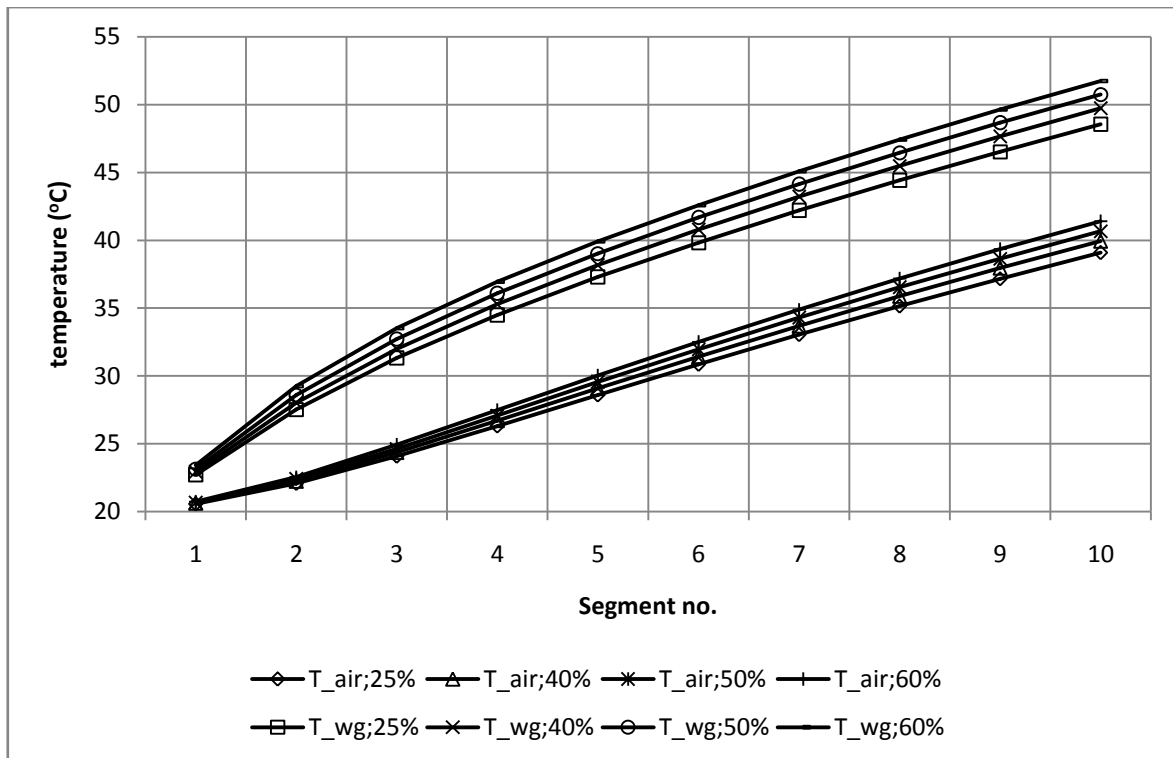


Fig.17.Segment air and water-glycol temperature profiles for varying concentration

Similar results have been obtained for other plate spacing's namely 50mm and 500mm are shown in figure 18. The spacing and concentration were kept constant at 20mm and 40% respectively.

The next results are for optimization of the draft height. The draft height was varied from 1m to 20m and the results

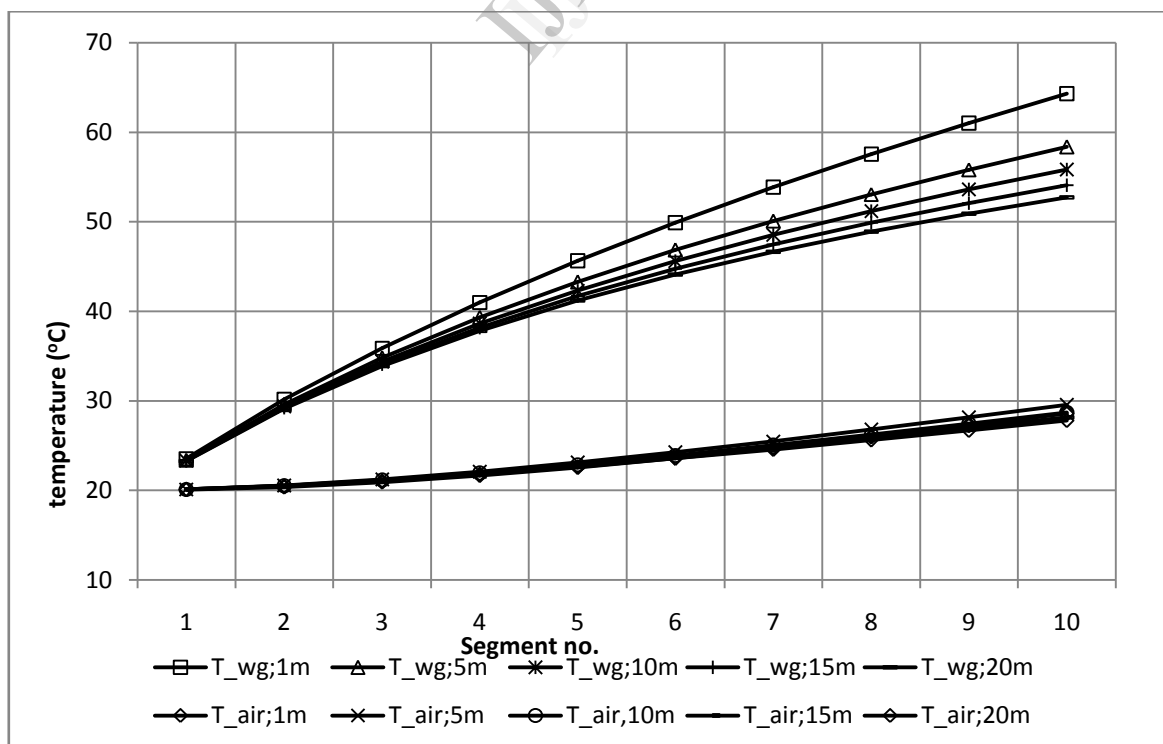


Fig. 18.Segment air and water-glycol temperature profiles for varying draft height

## X. ANALYSIS AND DISCUSSION

The performance of the storage model is shown in figures 12 and 13.

- Air heating is maintained as indicated by the continuously higher temperature of air above the ambient temperature;
- Storage build-up shown by the continuous build-up of the storage or tank temperature; and
- Reversal of energy transfer between the storage/tank and the water ethylene glycol in the collector shown by the temperature profiles crossing-over from the solar hours to the non-solar hours; this is shown in the magnified sector of figure 12 in figure 13 below where the tank temperature is now the highest followed by the temperature of the water ethylene-glycol in the collector and finally by the absorber temperature.

The optimisation aspect of the research is shown in figures 14 to 17. Air temperatures at different segments with varying air gaps are shown in figure 14. Temperatures with the minimum possible air gap of 5 mm were the highest as expected. Increase in air gap results in lower temperature at all segment numbers. Likewise, temperature at different segments for ethylene-glycol mixture and varying air gaps are shown in figure 15. The water ethylene glycol temperature profiles are higher at higher air gap values than at lower air gap values. Segment air and water-glycol temperature profiles for varying concentration for 5 mm air gap are plotted together in figure 16. It is observed that the temperature of air is generally lower than the temperature of water ethylene-glycol. This is possibly due to higher thermal conductivity of water; the same trend was observed with 50 mm air gap and 500 mm air gap. The temperature profiles for both flow streams are higher with higher concentration levels of the heat storage fluid. Figure 17 shows that the temperature profile for the air flow attains maximum values at the draft height of 5m and reduces when the draft height is lower or higher than 5m; this phenomenon requires further scrutiny.

## XI. ECONOMIC CONSIDERATIONS

The economic analysis can be presented in two formats: as a financial analysis using the cost-benefit analysis metrics of benefit-cost ratio (BCR), return on investment (ROI), and net present value (NPV); or in a descriptive manner outlining the local relevance of the research. In this particular case it is found that the local context far outweighs any financial analysis that maybe conducted is more driven by the higher energy poverty currently being experienced in the sub-region. More information is required in order to undertake a financial benefit analysis: in particular the total investment cost,  $I_{TOTAL}$ , of the solar air heater is a sum of costs of all its components:  $C_{COLLECTOR}$ , cost of solar collector,  $C_{STORAGE}$ , cost of storage tank,  $C_{HTF}$ , cost heat transfer fluid (HTF) and  $C_{PIPING}$ , cost of piping.

$$I_{TOTAL} = C_{COLLECTOR} + C_{STORAGE} + C_{HTF} + C_{PIPING} \quad (29)$$

This information together with monetized benefits of the project maybe used to determine each of the following:

Benefit-Cost Ratio:

$$BCR = \frac{\text{Total Discounted Benefits}}{\text{Total Discounted Costs}} \quad (30)$$

Return on Investment; (%):

$$ROI = \frac{(\text{Total Discounted Benefits} - \text{Total Discounted Costs})}{\text{Total Discounted Costs}} \quad (31)$$

Net Present Value:

$$NPV = \text{Total Discounted Benefits} - \text{Total Discounted Costs} \quad (32)$$

These will be undertaken in a future study; for now it suffices to say: The concept of affordable solar thermal storage has been identified as one critical factor that could promote the adoption of solar energy usage; solar energy resource, despite being one of the best globally, remains largely untapped. Access to electricity in the Southern African sub-region is very low except for a few countries as shown in fig. 19 below. Only three countries have access to electricity significantly above the average for Sub Saharan Africa which is 17%, Mauritius, South Africa and Zimbabwe. [15]

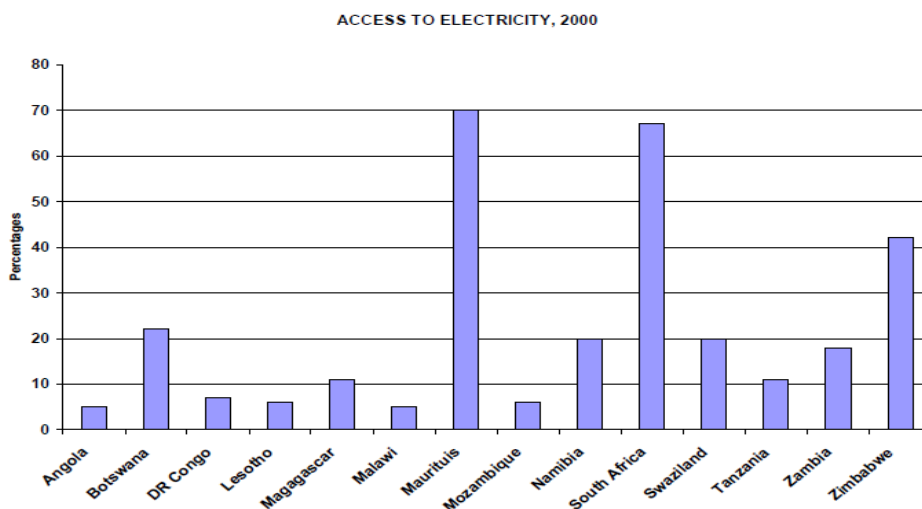


Fig. 19. Access to electricity by country in Southern Africa

## XII. CONCLUSIONS

This work involved designing a novel method of simultaneously heating air for space heating or any other suitable application while at the same time heating a liquid sensible storage media for use during non-solar hours. It was initiated as an off-shoot project of an updraft solar chimney project for electricity generation; however upon an extensive survey as well as a detailed review of the solar chimney project it was found not to be viable, at least in the time being until more innovative and cost effective structural materials and construction methods are developed. The storage model was however considered adequate for other applications such as space heating, crop drying etc. A concept was developed followed by mathematical models and computer simulations; and finally a prototype was constructed. Preliminary trials were conducted on the prototype; however, due to the dissolution of the client company extensive trials remain outstanding.

Maximum temperatures attained were 75.3°C, 74.6°C, 48.8°C and 31.9°C respectively for the absorber, heat transfer fluid in the collector, heat transfer fluid in the storage tank, and air flow at the exit of the collector; the ambient temperature varied from 13°C to 29°C.

The results show a gradual growth in the storage temperature as indicative of the technical viability of the developed process. The results have also shown the reverse-thermosyphon effect through the reversal of the direction of the heat transfer from the storage to the air flow path during the non-solar hours. The varying in performance for different values of the variable parameters indicates the need for further optimization of the model. For the given storage design, the best performance parameters for both air heating and storage fluid heating maybe summarised as plate spacing of 5mm, glycol-water concentration of 60% and draft height of 5m. Further studies are recommended on optimisation and optimum design and extensive testing of the solar air heater systems with natural draft. A through economic analysis is also outstanding but the project is generally acceptable based on the need to develop clean energy technologies that also yield environmental benefits and encourage tapping into the abundant solar energy resources.

## ACKNOWLEDGEMENTS

The Consultants wish to acknowledge the contribution of several other colleagues from the University of Botswana, the University of KwaZulu-Natal, University of Stellenbosch and the Botswana Technology Centre (BOTECH), who have tendered valuable suggestions and interacted with the Consultants during the progress of the work and in the formal presentations at BOTECH.

## REFERENCES

- [1] <http://www.botec.bw/index.php/botec-projects/energy/the-solar-chimney> accessed July 29, 2013
- [2] <http://inventors.about.com/od/timelines/a/Photovoltaics.htm>
- [3] <http://exploringgreentechnology.com/solar-energy/history-of-solar-energy/>
- [4] <http://solarwall.com/media/images-main/2-products/brochure/SolarDuctSpec.pdf>
- [5] [http://weather.uk.msn.com/monthly\\_averages.aspx?wealocations=wc:BCXX0001](http://weather.uk.msn.com/monthly_averages.aspx?wealocations=wc:BCXX0001)
- [6] Sharma Atuletal, Review on thermal energy storage with phase change materials and applications: *Renewable and Sustainable Energy Reviews* 13 (2009) pp 318-345
- [7] Morrison G.L., Reverse Circulation in Thermosyphon Solar Water Heaters, *Solar Energy* Vol. 36, No. 4, pp. 377-379, 1986
- [8] Incropera P Frank et al, 2007: Fundamentals of Heat and Mass Transfer; John Wiley & Sons; USA, ISBN \*978-0-471-45728-2
- [9] <http://www.jgsee.kmutt.ac.th/exell/Solar/FlatPlate.rtf>
- [10] Duffie J.A., Beckman W.A., "Solar Engineering of Thermal Processes" 2nd Ed., John Wiley & Son, Inc., USA, 1991 ISBN 0-471-51056-4 p281
- [11] Rabadiya A.V., Kirar R., Comparative Analysis of Wind Loss Coefficient (Wind Heat Transfer Coefficient) For Solar Flat Plate Collector; in International Journal of Emerging Technology and Advanced Engineering Website; (ISSN 2250-2459, Volume 2, Issue 9, September 2012) 463; [www.ijetae.com](http://www.ijetae.com)
- [12] Klein S.A., Alvarado F.L., EES, Engineering Equation Solver for Microsoft Windows Operating Systems, F-Chart Software, Middleton, WI 53562, USA, 1992-98
- [13] Situmbeko S.M., Kumar K.L., BOTECH Solar Thermal Storage Model Final Report, 2013.
- [14] <http://www.timeanddate.com/weather/botswana/gaborone/hourly> (2012)
- [15] <http://www.afrepren.org/project/gnesd/esdsi/erc.pdf>